Dear Author,

Please, note that changes made to the HTML content will be added to the article before publication, but are not reflected in this PDF.

Note also that this file should not be used for submitting corrections.

Optics Communications ∎ (∎∎∎∎) ∎∎∎–∎∎∎

Contents lists available at ScienceDirect

Optics Communications

journal homepage: www.elsevier.com/locate/optcom

1.25–3.125 Gb/s per user PON with RSOA as phase modulator for statistical wavelength ONU

Q1 Guang Yong Chu, Victor Polo, Adolfo Lerín, Jeison Tabares, Iván N. Cano, Josep Prat *

Departament de Teoria del Senyal i Comunicacions, Universitat Politècnica de Catalunya, 08034 Barcelona, Spain

ARTICLE INFO

Article history:
Received 7 May 2015
Received in revised form
27 July 2015
Accepted 18 August 2015

Keywords:
Coherent communications
Fiber Optics Communications
Fiber optics links and subsystems
Phase modulation

ABSTRACT

We report a new scheme to support, cost efficiently, ultra-dense wavelength division multiplexing (UDWDM) for optical access networks. As validating experiment, we apply phase modulation of a reflective semiconductor optical amplifier (RSOA) at the ONU with a single DFB, and simplified coherent receiver at OLT for upstream. We extend the limited 3-dB modulation bandwidth of available uncooled To-can packaged RSOA (~400 MHz) and operate it at 3.125 Gb/s with the optimal performance for phase modulation using small and large signal measurement characteristics. The optimal condition is selected at input power of 0 dB m, with 70 mA bias condition. The sensitivities at 3.125 Gb/s (at BER$=10^{-3}$) for heterodyne and intradyne detection reach −34.3 dB m and −38.8 dB m, respectively. Q2

1. Introduction

The wavelength-division-multiplexed passive optical network (WDM-PON) has been considered as an ultimate solution for the next-generation access network capable of providing unlimited bandwidth to each user [1]. However, if WDM-PON technologies are directly applied for massive deployment, it would be extremely complex, and the potential WDM-PON is to be integrated and improved [2]. Plenty of scientists have believed that it is crucial to increase the operating speed and maximum reach of WDM-PON, while it has no sense if people achieve them without affordable cost [1–3]. In order to apply them cost-efficiently, the system should require colorless optical network units (ONUs). It is desired that the whole system use modulators of low consumption, even limit the number of amplifiers [2,3]. For bidirectional transmission the Rayleigh backscattering (RB) would limit the performance if we want to reuse the carrier from optical line terminal (OLT) [4].

On one side, some researches on reusing the wavelength from OLT via semiconductor optical amplifier (SOA), reflective SOA (RSOA), and SOA integrated with reflective electro-absorption modulator (SOA-REAM) [5–8] have been done, while power penalty is the serious problem for these applications. Hence, there is an idea for limiting the power penalty to put the laser at ONU side, such as tunable laser at ONU [10], however, it is too expensive to deploy at each ONU. It is to be expected the laser at ONU is effectively used. Both downstream and upstream, using phase modulation, present better performances than that of intensity modulation for upstream.

On the other side, coherent detection is used at the receiver side to achieve a link budget of beyond 40 dB, which is superior to any existing direct detection based technology, and which can be utilized either for long reach or splitting factors extensions [9–11]. Coherent detection has been confirmed that it can improve the sensitivity and the spectrum efficiency in access network [12,13]. Compared with homodyne detection, heterodyne detection presents inherent image frequency interference, and as a result homodyne/intradyne reception is considered a better solution [14].

With this aim, first we simplify the hardware by applying the laser at ONU with the functions of both uplink's carrier and downlink's local oscillator laser (LO). These components can be integrated in a low footprint monolithic chip at ONU for each user.

This paper is organized as follows: a bidirectional schematics with single distributed feedback laser (DFB) based ONU is brought forward in Section 2, and optimization of operating condition for phase modulation is given in Section 3, validating tests both for small signal and large signal are demonstrated in Sections 4 and 5, respectively.

2. Bidirectional UDWDM subsystem and structure

Traditional intensity or phase modulator is based on $LiNbO_3$ architecture, but it presents the issues of large footprint, high optical losses, high-power consumption and integration

* Corresponding author.
E-mail address: jprat@tsc.upc.edu (J. Prat).

http://dx.doi.org/10.1016/j.optcom.2015.08.046
0030-4018/© 2015 Published by Elsevier B.V.

Table 1
Comparison between traditional $LiNbO_3$ modulator and RSOA.

	$LiNbO_3$ phase modulator	RSOA
Modulator length (L)	$5\ \text{cm} \le L \le 10\ \text{cm}$	$0.3\ \text{mm} \le L \le 1.6\ \text{mm}$
Modulator width (W)	$2\ \text{cm} \le W \le 5\ \text{cm}$	$0.2\ \text{mm} \le W \le 0.5\ \text{mm}$
RF driving signal (V_0 or I_0)	$4\ \text{V} \le V_0 \le 6\ \text{V}$	$10\ \text{mA} \le I_0 \le 70\ \text{mA}$

compatibility with the laser, thus not being suited for fiber-to-the-home (FTTH) ONUs. Semiconductor integration, like InP RSOA, is a way to facilitate the design of complex photonic circuits with multiple photonic functions [15].

A comparison between the traditional phase modulator ($LiNbO_3$) and the RSOA is given in Table 1; the parameters are from the references [16–18]. The RSOA presents the benefits both on the size and the injected driving signal.

We propose the network schematic as shown in Fig. 1. The upstream data use the RSOA as a phase modulator for reducing the power consumption, and it is expected that the laser will be integrated for both RSOA (as the upstream carrier) and receiver (as the LO) at ONU. At OLT side, in order to receive the upstream data, coherent detection is also used for improving the sensitivity of the receiver. The advantage of additional sensitivity can be used for power splitting losses and longer reach ultra-dense WDM-PON (UDWDM-PON). We focus on the upstream direction in this paper.

As previous explanation, the RSOA could be a low cost solution, while, it is not an easy goal to increase its maximum reach and operating speed. To improve these, we generate differential phase shift keying (DPSK) signal by directly modulating the RSOA. Once the RSOA is directly modulated, both the amplitude and phase of the output signal are modulated at the same time [19]. However, the undesired residual Amplitude Modulation (AM) and polarization dependency distort the signal and degrade the sensitivity of the receiver, which will be described in next section. Based on these reasons, the optimal operation region should be found in order to operate it efficiently.

3. Optimization of RSOA for phase modulation

In order to be operated at the best condition for the phase modulation, the gain, the optical-signal-to-noise-ratio (OSNR), amplified spontaneous emission (ASE) noise and the polarization dependent factors are required to be considered. The method for optimizing phase region consists of tuning both input power and bias current to achieve the minimum residual AM component and the polarization sensitivity. The optimal condition should have a better performance of phase modulating efficiency (PME).

The equation for gain measurement is as follows [19]:

$$G = 10\lg\frac{P_{out}^{s}}{P_{in}^{s}} = 10\lg\left(\frac{P_{out}-P_N}{P_{in}-P_{sse}}\right) \tag{1}$$

where P_{out}^{s} and P_{in}^{s} are the pure output power and input power of RSOA, respectively. P_{out} and P_{in} are the measured output and input powers, P_N represents the noise power, P_{sse} is the source spontaneous emission power of the laser in the experiment.

The room temperature of the RSOA is around 27 °C. Measured gain and OSNR are shown in Fig. 2(a). The maximum gain of the RSOA is about 21 dB, and the modulation region is between −10 dB m and 0 dB m. OSNR factor would be increased by injecting more optical power. The output power of the RSOA influences the signal quality at the receiver side, the increasing power goes to the linear region from −30 dB m to −10 dB m, and nearly flat region between −10 dB m and 0 dB m. The output power which directly influences the received performance of modulation, is increased by the input power and the injected current as shown in Fig. 2(b). At the same time, with a laser after amplifier, the ASE power (P_{ASE}) of RSOA is the main noise for RSOA [19]. From Fig. 2 (b), the ASE would be limited by increasing the input power [20,21].

$$P_{ASE} = P_N - G{\cdot}P_{sse} \tag{2}$$

Considering both the noise and output power of the RSOA, 0 dB m presents the optimal condition that minimizes the residual AM. While, for higher than 0 dB m of input power, the laser has a high consumption and it is not suitable for low cost ONU. It is because that we need the laser at ONU, and split the power both for RSOA and coherent detection at ONU for colorless ONU, all the component is required monolithic integrated chip.

As previously mentioned, when directly modulating the RSOA, the AM component would degrade the performance of DPSK detection. Hence, besides input power, we also need to select the bias current for RSOA in order to limit the tiresome AM component. The measured output power under different bias condition is shown in Fig. 3. Clearly, the 70 mA current is the ideal condition for phase modulation which the amplitude component would

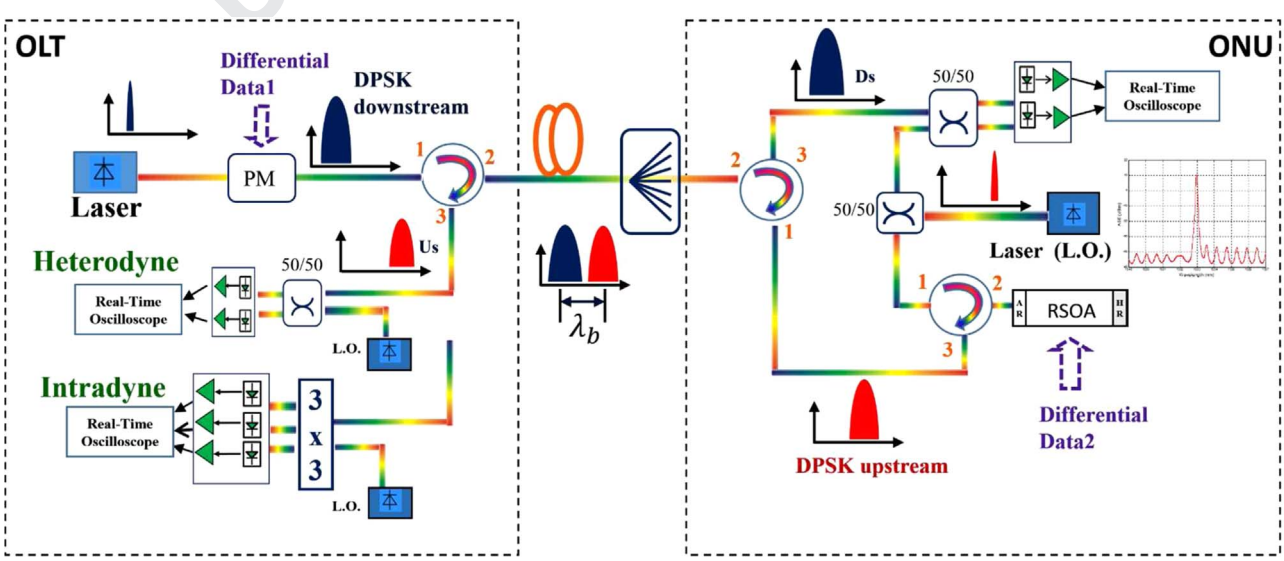

Fig. 1. Proposed subsystem of DPSK–DPSK bidirectional transparent UDWDM-PON (inset shows the spectrum of DFB at ONU).

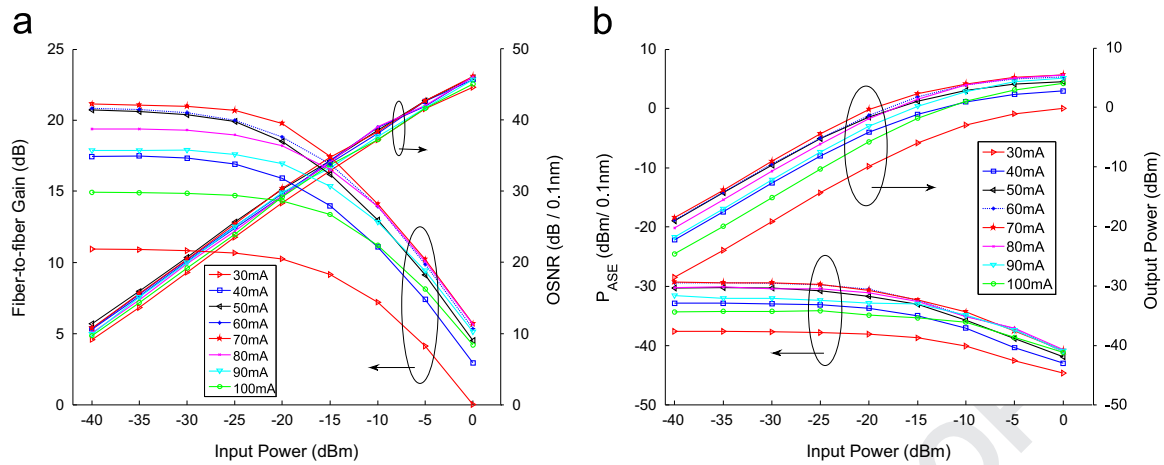

Fig. 2. (a) Measured gain and OSNR versus optical input power. (b) Measured ASE power spectral density and output power versus optical input power.

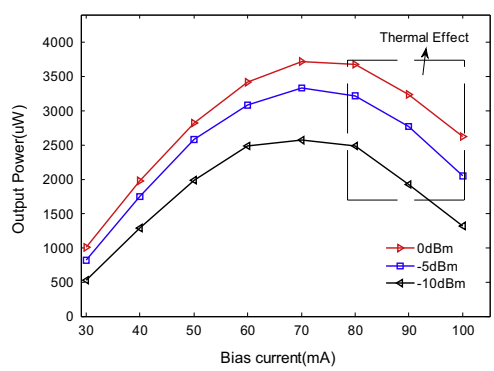

Fig. 3. Measured output power versus bias current under different input power (0 dB m, −5 dB m, and −10 dB m).

maintain the same value, and it would give a stable performance when the signal is introduced to the RSOA.

Another important physical issue in coherent detection is the fast polarization changes at the input of the receiver that influences not only the sensitivity but also the demodulation performance. Polarization changes originate both from the signals propagation along the fiber as well as the RSOA structure. In this case, we can limit the RSOA's polarization influences for available To-can packaged RSOA via characterization's measurement (at some region, RSOA is sensitivity for polarization) for the purpose of obtaining the polarization mitigation on the whole link. As we explained previously, the AM component influences the performance of phase modulation, we have found the best operation point at 70 mA with input power of 0 dB m. However, when the component is modulated in phase with coherent detection, the polarization deviation of the RSOA would influence the phase modulation. It is because that the RSOA's polarization dependent gain (PDG) would be different, which would make the AM component always changing. The deviation of the AM component changing by time can cause degradation on the system performance seriously.

The origin of PDG in RSOA is due to the fact that bulk active material has much larger transverse electric (TE) amplification than transverse magnetic (TM), on account of the different confinement factors [21,22]. To compensate for the birefringence, the strain [23] in the active material enhances the gain of TM with respect to TE, making the RSOAs less polarization dependent. However, this balance does not entirely mitigate PDG [24] and depends on input power, gain, bias current, and wavelength. The wavelength for UDWDM-PON is selected by the structure, for previous results, we have selected the bias current (70 mA) for phase modulation with the advantage of minimizing residual AM component, however both the residual AM and polarization dependent output power are dependent by the optical input power. Based on previous measurements (Fig. 2), higher input power in saturation region can limit the residual AM, then the polarization insensitivity region is required to be selected.

The measured polarization dependent results are shown in Fig. 4. Fig. 4(a) shows the gain at TE mode and TM mode at the same bias condition (70 mA). Fig. 4(b) shows the polarization dependent gain influenced by the input power of RSOA. The PDG is the lowest (around 0.1) when the input power is around −5 dB m.

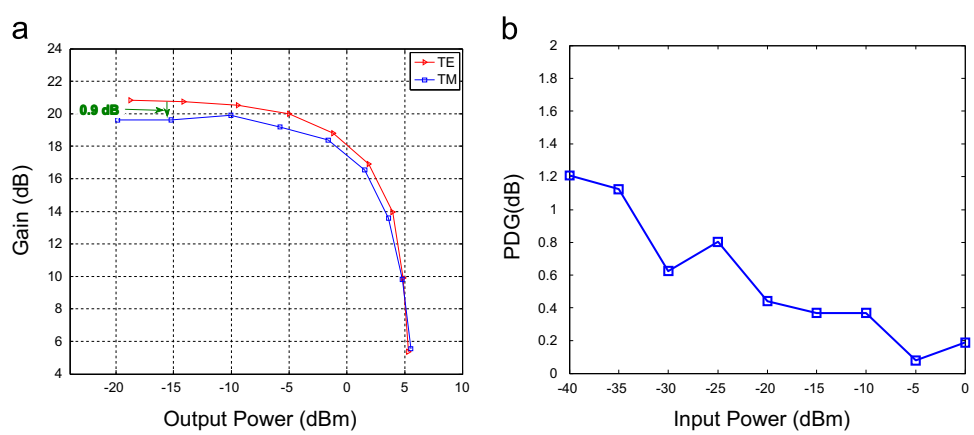

Fig. 4. (a) Gain versus output power at different polarization mode (b) PDG against input power at 70 mA, 0 dB m.

Please cite this article as: G.Y. Chu, et al., Optics Communications (2015), http://dx.doi.org/10.1016/j.optcom.2015.08.046

The PDG is 0.3 at the input power of 0 dB m.

In summary, balancing between minimizing the residual AM and polarization dependency, the condition of P_{in}=0 dB m, I_{bias}=70 mA is considered as the optimal operating points.

4. Validating for small signal measurement

In order to validate the performance, the RSOA is tested in small signal response via network analyzer. The measurement of Frequency Modulating Efficiency (FME) and PM Efficiency (PME) use the linear transfer function of an optical filter as shown in Fig. 5(a). It is assumed that the filter transfer function is linear to the frequency (ω_p) around the carrier frequency (ω_0) [25].

The transfer function can be represented as [25]

$$H(\omega_p) = T_0[1 + c_1(\omega_p - \omega_0)] \tag{3}$$

where T_0 is the amplitude transmission and c_1 is the differential coefficient at around ω_0.

Based on Fourier analysis, the approximated optical-power waveforms after propagation through the filter can be derived as

$$P_{left} \approx T_0^2 P_{in}\left(1 - 2c_1\frac{d\phi}{dt}\right),\ P_{right} \approx T_0^2 P_{in}\left(1 + 2c_1\frac{d\phi}{dt}\right) \tag{4}$$

here, P_{left} is the output power when the filter slope is at the left side, and P_{right} is the output power when the filter slope is at the right side. Then,

$$P_{AM} = \frac{P_{left} + P_{right}}{2} = T_0^2 P_{in},\ P_{FM} = \frac{P_{left} - P_{right}}{2} = 2T_0^2 P_{in} c_1 \frac{d\phi}{dt} \tag{5}$$

FM/*AM* has the relation with the phase shift component,

$$\frac{P_{FM}}{P_{AM}} = 2c_1 \cdot \frac{d\phi}{dt} \tag{6}$$

and the frequency deviation is as follow:

$$\Delta\upsilon = \frac{1}{2\pi}\cdot\frac{d\phi}{dt} = \frac{1}{2\pi}\cdot\frac{1}{2c_1}\cdot\frac{P_{FM}}{P_{AM}} \tag{7}$$

For small signal modulation, FM Efficiency is given by

$$\delta\upsilon(\omega) \equiv \delta\bar{\upsilon}(\omega) \approx \frac{1}{2\pi}\cdot\frac{1}{2c_1}\cdot\frac{\delta P_{FM}(\omega)}{P_0} \tag{8}$$

and $\delta\upsilon$ has the relationship with $\delta\phi$,

$$\delta\phi = 2\pi\int\delta\upsilon\cdot dt \tag{9}$$

Based on Fourier Transform, PM Efficiency is

$$\delta\phi(\omega) = \frac{2\pi}{j\omega}\delta\upsilon(\omega) \tag{10}$$

The frequency responses are measured at the bias condition from 40 mA to 70 mA; and the input power for the RSOA is now maintained at 0 dB m. The AM response and the FM Efficiency are shown in Fig. 6(a). It shows that the limited 3-dB bandwidth (BW) is limited to around 0.4 GHz, increasing from 40 mA to 70 mA; the FM Efficiency is measured in frequency domain with maximum at 500 MHz/mA when the bias current is 70 mA. The PM Efficiency, shown in Fig. 6(b), is calculated by the FM Efficiency from Eq. (10), presenting a flat and smooth curve appears at low frequency range at 70 mA.

In order to obtain accurate results for small signal chirp parameter, fiber dispersion should be accurately and independently measured [26]. The chirp parameter is obtained by measuring the electro-optic (EO) response by inserting dispersive fibers between the modulator and the light-wave component analyzer (LCA) [26–28]. The interaction between fiber dispersion and modulator chirp results in resonance dips in the spectrum. The equation describing the resonance points and the chirp is written as [26]:

$$f_k^2 L = \frac{c}{2D\lambda^2}\left(1 + 2k - \frac{2}{\pi}\arctan\alpha\right) \tag{11}$$

$$\alpha = \tan\left[2\pi\left(1 - \frac{2f_0^2 DL\lambda^2}{c}\right)\right] \tag{12}$$

where α is the chirp parameter, f_k is the k-th order of resonance, D is the fiber dispersion, c is the speed of light and λ is the wavelength.

An experimental curve of Eq. (11) is illustrated in Fig. 7(a). By fitting the experimental resonance points, the chirp under different bias conditions is calculated and the result is shown in Fig. 7 (b). It indicates that the chirp parameter is around 1.34 under different bias currents.

5. Validating for large signal measurement with coherent detection

In order to give a clear evidence of the method effectiveness to search for the optimal phase modulating condition (I_{bias}=70 mA, P_{in}=0 dB m), we test the RSOA with 2 × 2 heterodyne detection and 3 × 3 intradyne detection (without phase lock loop) as shown in Fig. 8(a) and (b).

Based on the structure we proposed in Fig. 1 for UDWDM-PON, the DFB is biased at 90 mA under the temperature of 25 °C, the linewidth is 4 MHz [29]. As shown in Fig. 8(a), the attenuator is used to provide the correct input power (0 dB m) for the RSOA

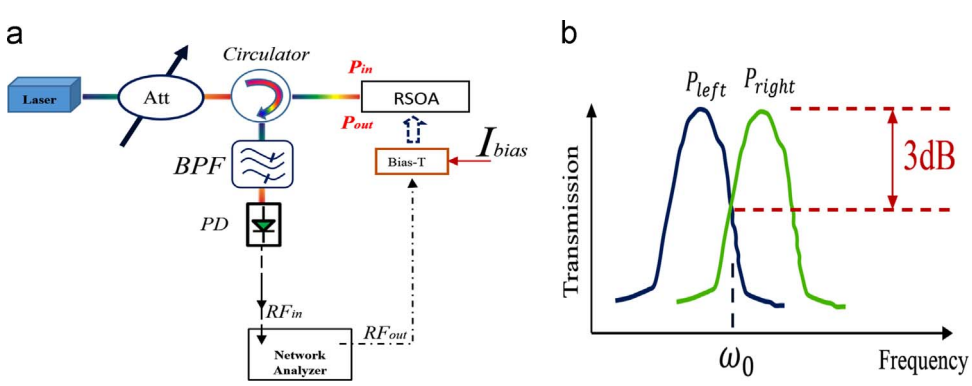

Fig. 5. (a) Experimental setup for FME and PME measurement using a band-pass-filter (BPF), and BPF is controlled by electrical voltage which can be maintain the stable measurement. (b) Explanation of measured transmission characteristics of a BPF, the transmission represents the square root of power loss.

Please cite this article as: G.Y. Chu, et al., Optics Communications (2015), http://dx.doi.org/10.1016/j.optcom.2015.08.046

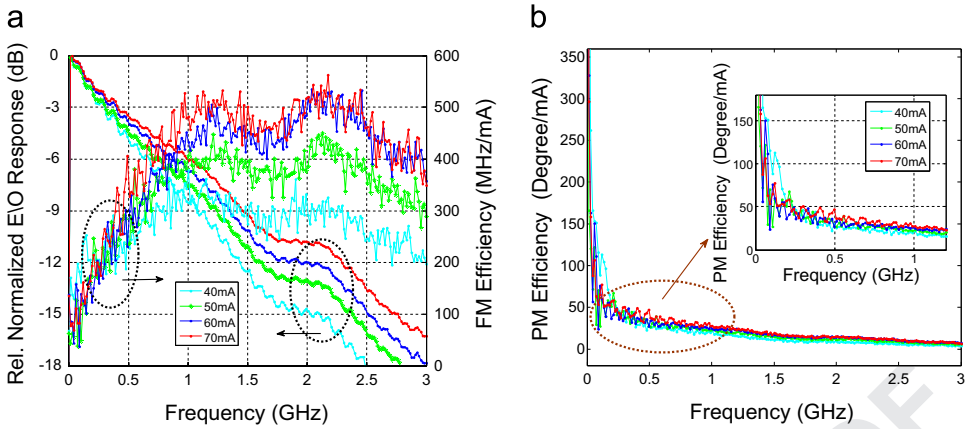

Fig. 6. (a) Normalized AM response and FM Efficiency at frequency domain (b) PM efficiency at frequency domain.

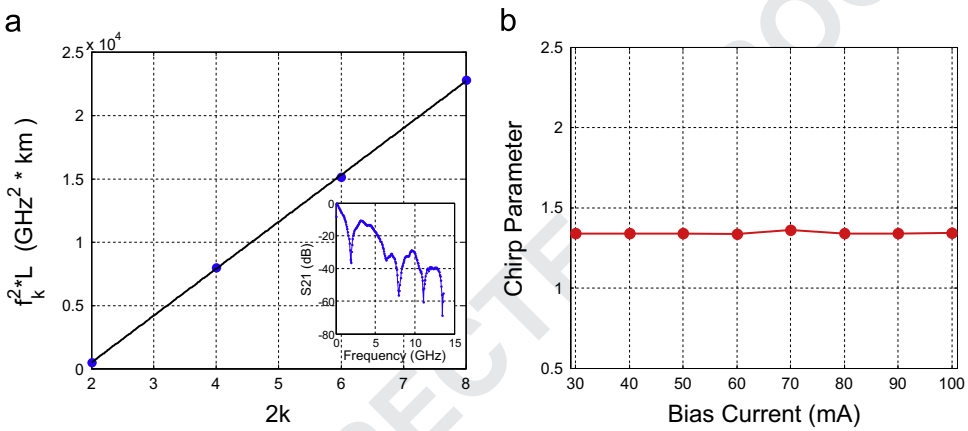

Fig. 7. (a) Measured resonant frequency at 70 mA bias condition for RSOA, where k is the k-th resonant position. Inset: measured chirp spectrum with 125 km SMF. (b) Chirp parameters at different bias conditions.

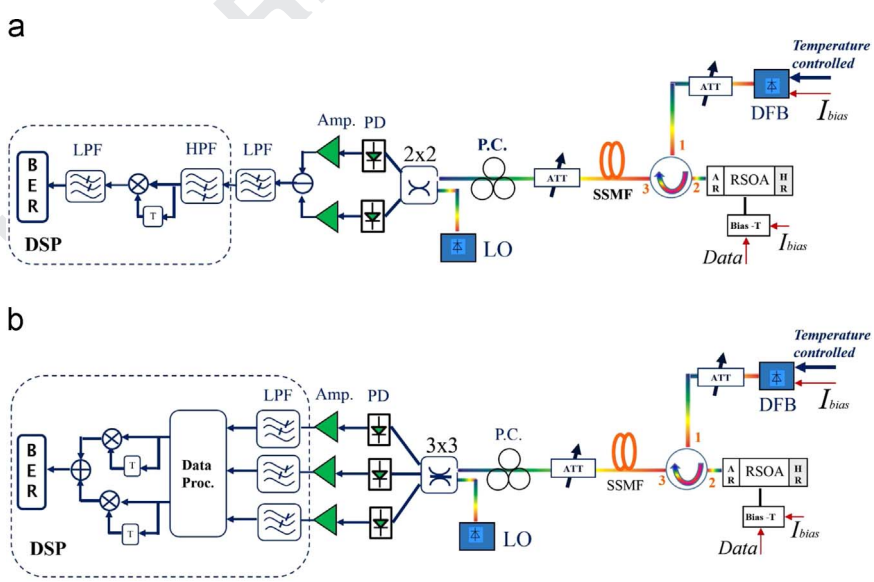

Fig. 8. Experimental setup for coherent detection. (a) Modulating RSOA in phase for balanced-PDs heterodyne detection. (b) Modulating RSOA in phase for 3 × 3 intradyne detection.

after the circulator, the transmitted data consisted of a non-return-to-zero (NRZ) pseudo random binary sequence (PRBS), which is grouped and stored in an arbitrary waveform generator (AWG) operating at different bit rates. The optical signal is then launched through 50 km of standard single-mode fiber (SSMF). The polarization controller (PC) compensated signal fluctuations due to state of polarization (SOP) changes in the fiber [30]. The received optical signal is converted to the electrical domain via photo-detectors (PD). Low noise amplifiers are used after PDs. The real-time oscilloscope resamples the electrical signal that is further digitally post-processed. The uncooled To-can packaged RSOA is tested at 1.25 Gb/s, 2.5 Gb/s, 3.125 Gb/s, respectively.

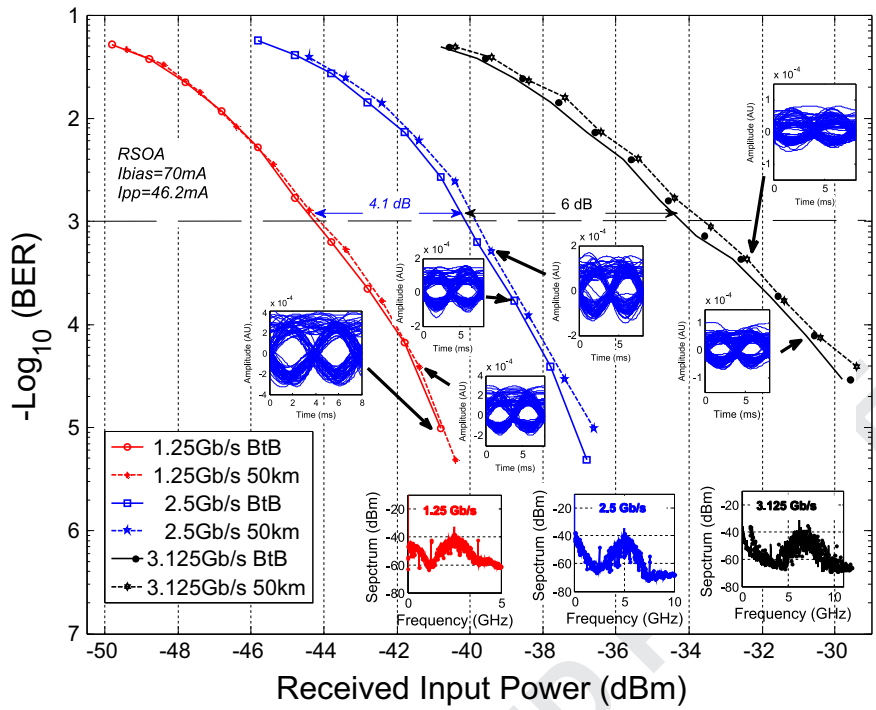

Fig. 9. BER versus optical received input power (2 × 2 heterodyne detection).

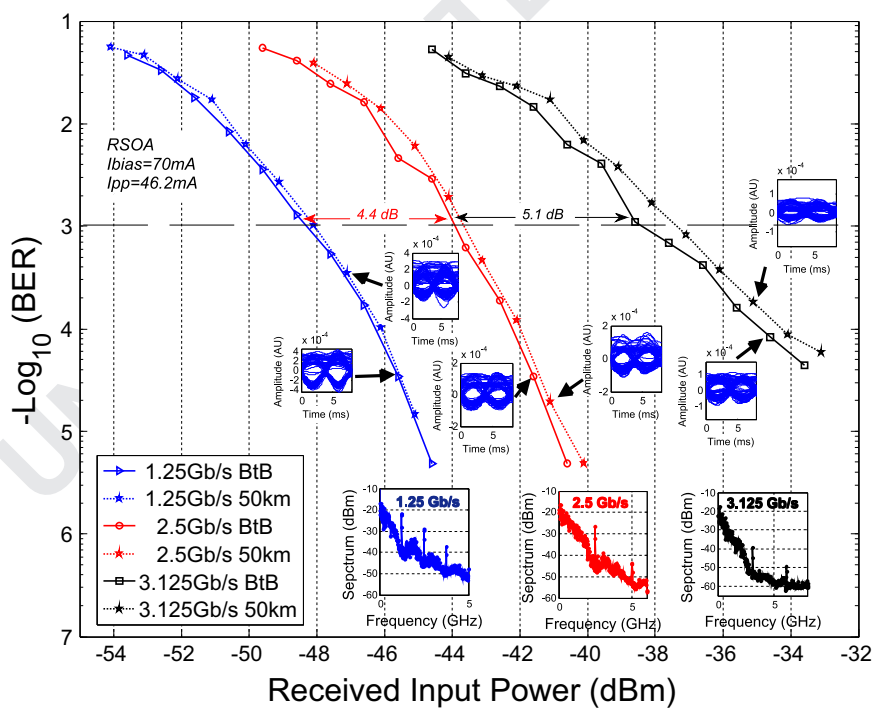

Fig. 10. BER versus optical received input power (3 × 3 intradyne detection).

The heterodyne receiver implemented is shown in Fig. 8(a). The electrical signal at the output of the photodiodes after amplifying is sampled with a 50 GSa/s real-time oscilloscope at 12.5 GSa/s with 10, 5, 4 samples per bit, respectively [12]. The intermediate frequency is selected at twice the bit rate. At digital signal processing (DSP), the electrical signal passes through a 1-bit delay and multiply block for differential demodulating after filtering. Before bit decision, the signal is filtered again with a 4 order butterworth low-pass filter (LPF). Finally, the bit error ratio (BER) is computed.

The BER is also measured with 3 × 3 intradyne detection as Fig. 8(b). Unlike the 2 × 2 heterodyne detection, we use 3 PDs to detect the received signal and obtain the I and Q components, and then use electrical amplifier (Amp.) to amplify the signal before DSP. 3 LPFs are used before data processing, then passed through a 1-bit delay and multiply block for differential demodulating, BER is tested after demodulating.

For heterodyne detection, the BER and the eye diagram are shown in Fig. 9. An input power of 3 dB m is provided by the ECL as LO. The results present the Rx sensitivities of −44.4 dB m, −40.3 dB m, and −34.3 dB m for back to back (BtB) transmission

(after 50 km fiber, the sensitivity arrives at −44.2 dB m, −39.7 dB m and −33.6 dB m) at BER$=10^{-3}$ for 1.25 Gb/s, 2.5 Gb/s, 3.125 Gb/s, respectively. At BER$=10^{-3}$, there are 4.1 dB power penalty between 2.5 Gb/s and 1.25 Gb/s, and 6 dB between 3.125 Gb/s and 2.5 Gb/s. The RSOA can be operated at the maximum bit rate of 3.125 Gb/s. The improved sensitivity can be used either for extended reach ONU or increased power splitting ratios in UDWDM-PON. Besides, the signal spectrum is also captured from the electrical spectrum analyzer (ESA) at different bit rates and intermediate frequencies as shown in the inset figure of Fig. 9.

The BER and the eye diagram are also tested via 3×3 intradyne detection (Fig. 10). Compared to 2×2 heterodyne detection or single-PD coherent detection, 3×3 intradyne detection has the theoretical 3-dB advantage of the sensitivity [12,30–33]. The RSOA is maintained at the same conditions compared with 2×2 heterodyne detection ($P_{LO}=3$ dB m). The results from the figure show that the sensitivity arrives at −48.2 dB m, −43.9 dB m, and −38.8 dB m for back to back (BtB) transmission (−48 dB m, −43.6 dB m and −37.4 dB m for 50 km fiber transmission) at BER$=10^{-3}$ for 1.25 Gb/s, 2.5 Gb/s, 3.125 Gb/s, respectively. The figure also shows that the power penalties are 4.4 dB and 5.1 dB at BER$=10^{-3}$ when increasing the bit rate 1.25 Gb/s to 2.5 Gb/s, and from 2.5 Gb/s to 3.125 Gb/s, respectively. It shows that the RSOA, which has the limitation of the modulating bandwidth of 400 MHz, is successfully tested at 3.125 Gb/s, with the advantage of optimizing the RSOA in phase modulation region.

6. Conclusion

We demonstrate an effective optimization of the RSOA for phase modulation through the measured characterization and best condition operation, with the purpose of minimizing the unwanted residual AM (for better BER) and polarization dependency (for long reach ONU). As validating tests with small signal measurements, we test that the FM Efficiency reaches 500 MHz/mA at the optimal bias of 70 mA. The results show that we could implement a long-reach UDWDM-PON operating at the speed for each user up to 3.125 Gb/s (using very low cost 0.4 GHz uncooled To-can RSOA), via coherent detection using 2×2 heterodyne and 3×3 intradyne receivers at the OLT, and digital signal processing techniques. Additionally, the downstream carrier and upstream carrier work at the same wavelength range, hence, it constitutes a simplified enabling technique towards Ultra Dense WDM-PON.

Acknowledgments

This work has been supported by European FP7 COCONUT Project (GA318515), the Ministry of Science and Innovation under Grant TEC2011-25215 (ROMULA) Project, and PhD fellowship donated by the China Scholarship Council (201207040059).

References

[1] J. Prat, Technologies for a cost-effective coherent udWDM-PON, in: Proceedings of OFC, Th3I, Los Angeles, 2015.
[2] Y.C. Chung, Future optical access networks, in: Proceedings of Proc. Signal Processing in Photonic Communications, JW1A.1, Colorado, 2012.
[3] M. Milosavljevic, P. Kourtessis, J.M. Senior, Wireless convergence over next generation OFDMA-PONs, in: Proceedings of ANIC, AWB3, Toronto, 2011.
[4] B. Schrenk, G. de Valicourt, J.A. Lazaro, R. Brenot, J. Prat, Rayleigh scattering tolerant PON assisted by four-wave mixing in SOA-based ONUs, IEEE J. Lightwave Technol. 28 (2010) 3364–3371.
[5] G. de Valicourt, D. Make, J. Landreau, M. Lamponi, G.H. Duan, P. Chanclou, R. Brenot, High gain (30 dB) and high saturation power (11 dB m) RSOA devices as colourless ONU sources in long reach hybrid WDM/TDM -PON architecture, IEEE Photon. Technol. Lett. 22 (3) (2010) 191–194.
[6] U.H. Hong, K.Y. Cho, H.G. Choi, Y.C. Chung, A simple carrier-phase estimation technique for high speed RSOA-based coherent WDM PON, in: Proceedings of OFC, OM2A.2, Anaheim, 2013.
[7] B. Schrenk, S. Dris, P. Bakopoulos, I. Lazarou, K. Voigt, L. Zimmermann, H. Avramopoulos, Flexible quadrature amplitude modulation with semiconductor optical amplifier and electroabsorption modulator, Opt. Lett. 37 (2012) 3222–3224.
[8] A. Naughton, C. Antony, P. Ossieur, S. Porto, G. Talli, P.D. Townsend, Optimisation of SOA-REAMs for hybrid DWDM-TDMA PON applications, Opt. Express 19 (26) (2011) B722–B727.
[9] F. Saliou, B. Le Guyader, L. Guillo, G. Simon, P. Chanclou, for G-PON, XG-PON1 and TWDM-PON co-existing on the same ODN, in: Proceedings of ECOC, Mo.4.1.2, Cannes, 2014.
[10] S. Smolorz, H. Rohde, E. Gottwald, D.W. Smith, A. Poustie, Demonstration of a coherent UDWDM-PON with real-time processing, in: Proceedings of OFC, PDPD4, Los Angeles, 2011.
[11] M. Morant, T. Quinlan, S. Walker, R. Llorente, Complete mitigation of brillouin scattering effects in reflective passive optical networks using triple-format OFDM radio signals, in: Proceedings of OFC, JWA072, Los Angeles, 2011.
[12] J. Prat, V. Polo, P. Zakynthinos, I. Cano, J.A. Tabares, J.M. Fàbrega, D. Klonidis, I. Tomkos, Simple intradyne PSK system for udWDM-PON, Opt. Express 20 (27) (2012) 28758–28763.
[13] M. Presi, F. Bottoni, R. Corsini, G. Cossu, E. Ciaramella, Low cost coherent receivers for UD-WDM NRZ systems in access networks, in: Proceedings of ICTON, MoC31, Graz, 2014.
[14] J.M. Fabrega, J. Prat, Homodyne receiver prototype with time-switching phase diversity and feedforward analog processing, Opt. Lett. 32 (5) (2007) 463–465.
[15] C. Kazmierski, D. Carrara, K. Lawniczuk, G. Aubin, J. Provost, R. Guillamet, 12.5 GB operation of a novel monolithic 1.55 μm BPSK source based on prefixed optical phase switching, in: Proceedings of OFC, OW4J8, Anaheim, 2013.
[16] X. Zhang, Amir Hosseini, X. Lin, H. Subbaraman, Ray T. Chen, Polymer-based hybrid-integrated photonic devices for silicon on-chip modulation and board-level optical interconnects, IEEE J. Sel. Topics Quantum Electron. 19 (6) (2013) 3401115.
[17] T. Kawanishi, T. Sakamoto, M. Izutsu, High speed control of lightwave amplitude, phase, and frequency by use of electro-optic effect, IEEE J. Sel. Topics Quantum Electron. 13 (1) (2007) 79–91.
[18] A. Meehan, M.J. Connelly, Experimental characterization and modeling of the improved low frequency response of a current modulated bulk RSOA slow light based microwave phase shifter, Opt. Commun. 341 (2015) 241–244.
[19] S.P. Jung, Y. Takushima, Y.C. Chung, Transmission of 1.25-Gb/s PSK signal generated by using RSOA in 110-km coherent WDM PON, Opt. Express 18 (14) (2009) 14871–14877.
[20] S. Jain, T.C. May-Smith, A. Dhar, A.S. Webb, M. Belal, D.J. Richardson, J.K. Sahu, D.N. Payne, Erbium-doped multi-element fiber amplifiers for space-division multiplexing operations, Opt. Lett. 38 (4) (2013) 582–584.
[21] J.C. Ribierre, G. Tsiminis, S. Richardson, G.A. Turnbull, I.D.W. Samuel, Amplified spontaneous emission and lasing properties of bisfluorene-cored dendrimers, Appl. Phys. Lett. 91 (2007) 081108.
[22] P.H. Lim, S. Park, Y. Ishikawa, K. Wada, Enhanced direct bandgap emission in germanium by micromechanical strain engineering, Opt. Express 17 (18) (2009) 16358–16365.
[23] M.J. Connelly, Theoretical calculations of the carrier induced refractive index change in tensile-strained InGaAsP for use in 1550 nm semiconductor optical amplifiers, Appl. Phys. Lett. 93 (2008) 181111.
[24] O.L. Ladouceur, K. Bergman, M. Boroditsky, M. Brodsky, Polarization-dependent gain in SOA-based optical multistage interconnection networks, IEEE J. Lightwave Technol. 24 (11) (2006) 3959–3967.
[25] K. Sato, S. Kuwahara, Y. Miyamoto, Chirp characteristics of 40-Gb/s directly modulated distributed-feedback laser diodes, IEEE J. Lightwave Technol. 23 (11) (2005) 3790–3797.
[26] F. Devaux, Y. Sorel, J.F. Kerdiles, Simple measurement of fiber dispersion and of chirp parameter of intensity modulated light emitter, IEEE J. Lightwave Technol. 11 (1993) 1937–1940.
[27] N. Courjal, J.M. Dudley, Extinction-ratio-independent method for chirp measurements of Mach–Zehnder modulators, Opt. Express 12 (3) (2004) 442–448.
[28] H.W. Chen, J.D. Peters, J.E. Bowers, Forty Gb/s hybrid silicon Mach–Zehnder modulator with low chirp, Opt. Express 19 (2) (2011) 1455–1460.
[29] H.W. Chen, Y.H. Kuo, J.E. Bowers, A hybrid silicon-AlGaInAs phase modulator, IEEE Photon. Technol. Lett. 20 (23) (2008) 1920–1922.
[30] I.N. Cano, A. Lerín, V. Polo, J. Tabares, J. Prat, Simple ONU transmitter based on direct-phase modulated DFB laser with heterodyne detection for udWDM-PON, in: Proceedings of ECOC, We.2.F.4., London, 2013.
[31] I.N. Cano, A. Lerín, M. Presi, V. Polo, E. Ciaramella, J. Prat, 6.25 Gb/s differential duobinary transmission in 2 GHz BW limited direct phase modulated DFB for udWDM-PONs, in: Proceedings of ECOC, P.7.2, Cannes, 2014.
[32] V. Polo, P. Borotau, A. Lerín, J. Prat, DFB laser reallocation by thermal wavelength control for statistical udWDM in PONs, in: Proceedings of ECOC, P.4.13., Cannes, 2014.
[33] V. Sales, J. Segarra, V. Polo, J. Prat, Statistical UDWDM-PONs operating with ONU lasers under limited tunability, IEEE Photon. Technol. Lett. 27 (3) (2015) 257–260.